Soil Dynamics and Earthquake Engineering 157 (2022) 107273

Contents lists available at ScienceDirect

Soil Dynamics and Earthquake Engineering

journal homepage: www.elsevier.com/locate/soildyn

Earthquake source effect and impact of the applied methodology to assess the overstrength factors of RC bridges

A.R. Sánchez [a], A. Arêde [b], J.M. Jara [a,*], P. Delgado [b,c]

[a] School of Civil Engineering, University of Michoacan, Morelia, Mexico
[b] CONSTRUCT-LESE, Faculty of Engineering (FEUP), University of Porto, Porto, Portugal
[c] proMetheus, Instituto Politécnico de Viana do Castelo, Rua Escola Industrial e Comercial Nun'Álvares, 4900-347, Viana do Castelo, Portugal

A B S T R A C T

Seismic hazard assessment in several sites worldwide depends on two or more seismic sources. Many countries affected by subduction zones have strong motions earthquakes originated in at least two important seismic sources. In Mexico, interplate earthquakes (subduction process) have epicenters located in the Pacific coast with hypocenter depths less than 45 km and intraplate earthquakes (intermediate-depth earthquakes) normally have epicenters inside the continent with depth hypocenters greater than 45 km. Both seismic sources can potentially produce events with magnitudes M_w greater than 8.0 and, therefore, generate severe damage to the country's infrastructure. The design process of the bridges in Mexico is based on the chapter of Seismic Design of the Manual of Civil Structures of the Federal Electricity Commission. The standard allows to reduce the spectral ordinates of the design spectra by ductility and overstrength. It establishes an overstrength factor of 1.5 to reduce the design spectra, value not well supported by the Manual. This study evaluates the effect of the seismic source and methodology used to compute overstrength factors of common typologies of reinforced concrete bridges. The seismic capacity of the bridges was calculated with nonlinear static analysis and nonlinear time history analysis. The results showed that the importance of the seismic source on the overstrength factors depends on the seismic location of the bridges and, in general terms, nonlinear static analysis overestimates the bridges overstrength.

1. Introduction

Most of the largest earthquakes and seismic energy dissipated in the world occurs in the Circum-Pacific Belt along the rim of the Pacific Ocean (interplate earthquakes). In Mexico, two seismic sources with independent occurrence processes control the seismic hazard. The subduction seismic source produces earthquakes with epicenters on the Pacific Coast in the West Country region. The second seismic source (normal-faulting inslab earthquakes) produces events of intermediate depth and the epicenters are normally inside the continent. Intraplate earthquakes have higher stress drop than interplate earthquakes and the seismic wave propagation produced in each seismic fault is different [1]. These authors found that deep-inslab earthquakes have large stress drops and they also exhibit fast attenuation. Both seismic sources, also found in many countries along the Pacific Belt, produce earthquakes that have historically caused damage to the Mexico's infrastructure. The difference of occurrence processes, the epicenter locations and their potentiality to generate strong motions encourage to evaluate the overstrength of bridges by independently considering two sets of accelerograms recorded in interplate and intraplate seismic movements.

Highway bridges are very important structures with a significant economic impact in case of an earthquake disaster. Currently, Mexico has more than 17,000 bridges in the National Highway Network and most of them are in seismic zones [2]. The chapter of Seismic Design of the Manual of Civil Structures of the Federal Electricity Commission [3], stipulates design spectra to design the bridges in Mexico. This document recommends an overstrength factor of 1.5 to reduce the design spectra for the seismic design of medium-span bridges. The following studies conducted in different countries show that overstrength factors depend on the seismic zone, bridge typology, piers height, among other factors that are not currently considered in the Manual. None of them analyzes the effect of the seismic source on the overstrength factors.

Bertero et al. [4]; suggested that one of the reasons of limited seismic damages observed after an earthquake occurrence is the structural overstrength. The overstrength comes from the real resistance of the structures, which is usually greater than the nominal resistance. Different studies suggest that the structural overstrength is related to the steel strength after the yield point, the increasing compressive strength of the concrete with time, the contribution of the slab to the beam strength, the yield of structural elements at different times, the minimum strength requirements indicated in regulations, the speed of load application, among others [5–9].

* Corresponding author.
E-mail address: jmjara70@gmail.com (J.M. Jara).

https://doi.org/10.1016/j.soildyn.2022.107273
Received 8 December 2021; Received in revised form 21 March 2022; Accepted 22 March 2022
Available online 30 March 2022

Concerning buildings, several authors have reported structural overstrength factors. Miranda and Bertero [10] found overstrength factors in the range of 2–5, based on the analysis of buildings in Mexico City. Particularly, the authors found relevant the infill masonry walls and the slab contribution in the structural overstrength. Shahrooz and Moehle [11] reported an overstrength factor of 7.7, in the experimental study of a 1:4 scale model of a six-story reinforced concrete (RC) building structure. Cassis and Bonelli [12] obtained overstrength values in the range of 3–5 from the study of RC structures with frames, walls and frame-wall systems, where frame structures presented the highest overstrength factor.

The building height is also important in the overstrength. Jain and Navin [13] found overstrength factors in the range of 2.8–12, in the study of RC buildings ranging from three to nine stories, located in India. Also, Massumi et al. [14] reported overstrength factors in the range of 2.1–5.5 for buildings with one to ten stories.

Mehanny and El Howary [15] analyzed 4- and 8-story moment frames in a moderate seismic zone. Using two different design approaches, one fulfilling the building code requirements and other by ignoring pre-specified constant acceleration lower bound when verifying drift demands. Based on pushover analysis the authors found overstrength factors in the range of 1.51–3.77. In tall buildings, Khy and Chintanapakdee [16]; studied a 39-story RC building to analyze the effect of floor slabs; the authors also found overstrength factors of 3.36 and 3.71 in both horizontal directions of analysis.

Kappos et al. [17] studied simply supported and continuous bridges located in an area of high seismicity in Europe. Based on pushover analysis, the authors found that the analysis direction is a relevant parameter. The authors reported overstrength factors in the range of 1.3–3.4 in the longitudinal direction and in the range of 1.2–5.8 in the transverse direction of the bridges.

Other studies proposed the seismic design of bridges by limiting overstrength factors. Awasthi et al. [18] designed a bridge curved in plan using different response reduction factors R and satisfying FEMA-356 performance-based criteria by keeping the overstrength factor below 2.0. The influence of pier overstrength on the Lead Rubber Bearings behavior was determined by Nobuyuki et al. [19]. The authors found negligible contribution, with the parameters used in the study, in a five-span isolated bridge.

Recently, Sánchez et al. [20] studied a set of reinforced concrete bridges with typical Mexican typology that are very common in other countries as well. The study determined overstrength factors of the bridges based on time-history analysis. The bridges were subjected to a set of 80 accelerograms. The selection of the seismic records was based on maximum spectral accelerations, regardless of the seismic source. In places affected by subduction seismic sources (interplate), there is also a seismic source that produces earthquakes within the interior of a tectonic plate with epicenters inside the continent (intraplate earthquake). The latter usually has epicenters closer to inhabited sites and to the infrastructure (bridges and buildings) of a country. These two seismic sources have independent occurrence processes, and, in Mexico, both have the potential to generate earthquakes with a magnitude greater than 8.0. Depending on the geographical distribution of the bridges, the seismic hazard can be governed by the two seismic sources or clearly by only one of them. Before recommending overstrength factors for the seismic design of RC bridges in an earthquake code in Mexico, it is required to analyze the influence of the seismic source of the selected accelerograms on the overstrength factors, particularly because there are groups of bridges controlled by one or another seismic source.

This study aims at studying the influence of the seismic source and the methodology used to assess overstrength factors of medium-span simply supported bridges formed by a deck of RC slab supported on prestressed beams. The substructure consists of RC single-column and multi-column piers. The bridges were subjected to a set of accelerograms from a subduction zone (interplate earthquakes) and to collected seismic records from intraplate earthquakes (normal-faulting inslab mechanism). Most of the studies to evaluate overstrength factors are based in pushover analysis. Besides evaluating the impact of the seismic source on the overstrength factors, this study analyzes the influence of the methodology used to compute the overstrength factors as well. To accomplish this objective, nonlinear static analysis and nonlinear dynamic analysis of the bridges were carried out.

2. Seismic sources

The Mexican Republic is geographically located in a zone of high seismicity and is part of the Pacific ring of fire. The subduction of the Pacific plate under the North American plate causes interplate and intraplate earthquakes. Both seismic sources have produced large tremors with devastating consequences in the country. Fig. 1 shows earthquake epicenters recorded in the period 1900–2020 originated in the interplate seismic source with $M_w \geq 7$ and epicenters in the intraplate seismic source with $M_w \geq 6$.

Both seismic sources have the potential to generate earthquakes with magnitude $M_w > 8$ and in last centuries several destructive earthquakes have struck the country. Interplate seismic sources, whose epicenters are in the Mexican Pacific coast, originate at depths less than 45 km and occur more frequently than intraplate tremors. The intraplate seismic source (normal-faulting mechanism) generates earthquakes with depth hypocenters greater than 45 km and are normally located inside the continent. A set of 45 accelerograms from each seismic source were selected and all seismic stations locate in hard soil sites, classified as soils with shear wave velocities $Vs > 700$ m/s.

Fig. 2 shows the response spectra of each seismic source for 5% of critical damping. Fig. 2a displays the response spectra of the seismic records of subduction earthquakes and Fig. 2b the response spectra of accelerograms generated in intraplate seismic sources. In both cases, the spectral mean (bold line) and the mean ± one standard deviation (dashed lines) of each group of spectra are also shown. Even though all the seismic stations are in hard soil sites, the spectral shapes of each group of response spectra are different. Earthquakes with origin in interplate seismic sources produced a mean spectrum that, after reaching the maximum amplitude, falls faster than the mean spectrum of events produced by intraplate movements.

The location of the earthquake epicenters of the two seismic sources makes more important the interplate earthquakes for the seismic behavior assessment of bridges located close to the Pacific coast, and the intraplate seismic source for bridges located inside the continent.

Currently, bridges in Mexico are designed with a force-based philosophy that uses overstrength factors to reduce the elastic design spectrum. In some countries, codes are migrating towards a performance-based design philosophy, which uses displacement-based design procedures. The design begins by selecting a target displacement with a more realistic estimate of the material strength in the inelastic range of behavior of structural elements [21], which reduces the impact of overstrength factors. Displacement-based design uses displacement response spectra. Fig. 3 shows the normalized pseudo-acceleration (Sa) and displacement (Sd) mean spectra of the suite of accelerograms collected from the two seismic sources. In the first case they were normalized with respect to the peak ground acceleration (PGA) and in the second case with respect to the maximum ground displacement (PGD). Interplate Sa spectra decay faster than intraplate seismic source and an appreciable difference in Sd spectra are also observed, particularly in the zone of fundamental periods of most of the bridges (between 1 and 3 s). These spectral shapes suggest a different effect of each group of accelerograms on the nonlinear seismic response of the bridges.

3. Numerical models

Most of the small and medium-span bridges in Mexico are RC superstructures supported on RC frame-type piers formed by one or more

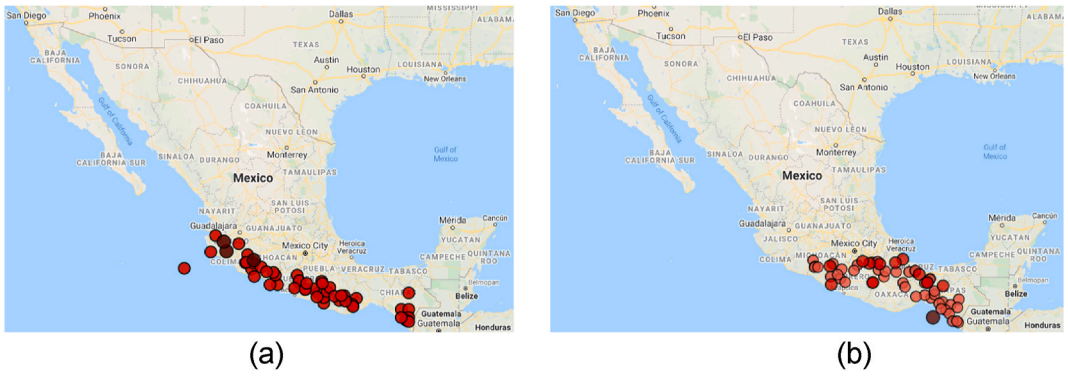

Fig. 1. Earthquake epicenters in Mexico during the period of 1900–2020. (a) Interplate earthquakes with $M_w \geq 7.0$ and (b) intraplate earthquakes with $M \geq 6.0$ (www.ssn.unam.mx).

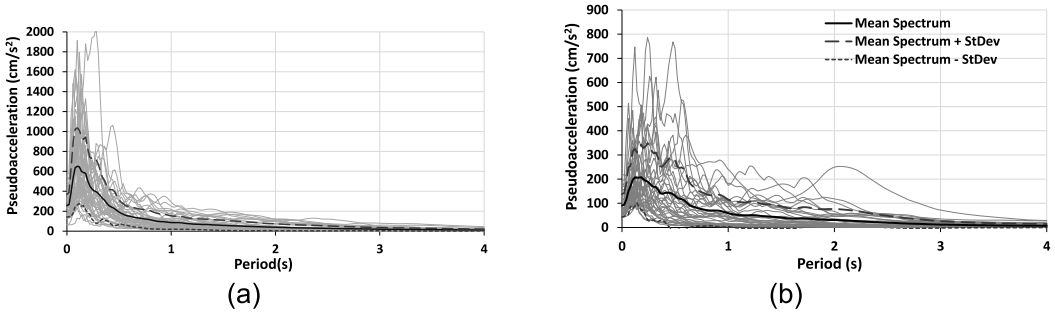

Fig. 2. Response spectra of accelerograms recorded in two independent seismic sources. (a) Interplate seismic source (subduction process) and (b) Intraplate seismic source (normal-faulting mechanism).

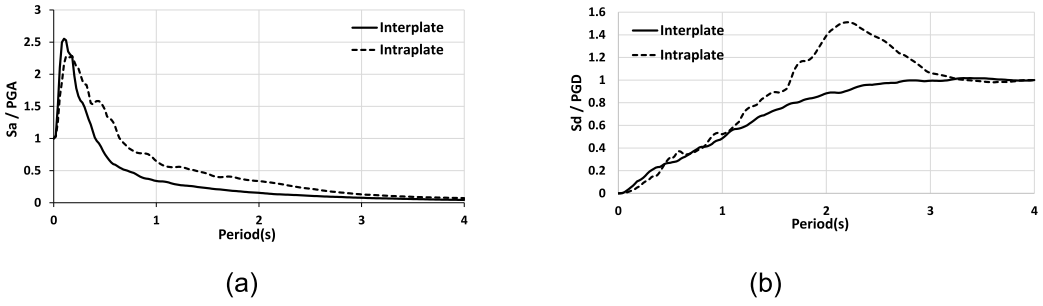

Fig. 3. Normalized response spectra for interplate and intraplate seismic sources. (a) Sa/PGA. (b) Sd/PGD.

columns. This study focuses on the group of bridges previously designed in the study of Sánchez et al. [20]; consisting of five-span simply supported RC bridges on multi-column (M) and single-column (C) RC piers. The deck is composed of a 0.20 m thick RC slab and prestressed concrete girders, resting on elastomeric bearings. The superstructure includes AASHTO type IV girders and Nebraska NU-2400 for the 30 m and 50 m

Fig. 4. RC bridges. (a) Single-column piers and (b) multi-column piers.

span bridges, respectively. Two types of substructures were included: single-column circular piers and four-column circular piers (Fig. 4). The bridges have piers' heights of 5 m, 10 m, 15 m and 20 m (P05–P20), and three possible location zones were considered concerning the seismic activity, namely: low seismicity (LS), medium seismicity (MS) and high seismicity (HS). The spectral accelerations in the plateau region of the design spectra were 0.60 g, 0.90 g and 1.56 g for LS, MS and HS seismicity zones, respectively.

The roadway is 9.60 m wide and the overall width of the bridge was 10.60 m. In the transverse direction, the bridges have RC 0.30 m width cross beams (diaphragms). The space between intermediate diaphragms is 1/6 L for the 30 m span bridges and 1/10 L for the 50 m span bridges. L is the span length.

Shell-type finite elements (quadrilateral elements with six degrees of freedom at each joint) were adopted to model the slab. Beams and columns are simulated by frame-type elements with six degrees of freedom per node. Two-nodes link type linear element, with six degrees of freedom per node were used to model the bearings, whereas nonlinear link elements (gap type) were adopted to model the expansion joints. The contribution of the abutment backfill was modeled using the recommendations of section 7.8.7 of Caltrans [22].

In all pier and abutments axes, there are 40 mm wide JCMY-55 expansion joints that separate slabs and beams from adjacent spans as evidenced in the numerical model detail included in Fig. 5. This numerical model does not include shear keys in the transverse direction and the elastomeric supports are composed of layers of Shore A-60 Neoprene (shear modulus of G = 1.0 MPa) and steel plates. The bearing dimensions (in millimeters) were in the range of 300 × 300 × 41-400 × 400 × 185 (length x width x thickness) as a function of the span length. The bearing lateral stiffness was in the range of 1.07–2.0 kN/mm and the vertical stiffness in the range of 324 kN/mm-510 kN/mm.

All RC elements of the superstructure and substructure were designed using a concrete compressive strength f'c = 24.5 MPa and elastic modulus Ec = 4400(f 'c)$^{1/2}$. Reinforcing steel has a modulus of elasticity Es = 205940 MPa and the yield strength fy = 412 MPa.

The trucks used to design the bridges were: HS20 (32.8 t), T3S3 (46.25 t) and T3S2R4 (72.5 t). More details of the load combinations, circulation lanes and design assumptions are described in Sánchez et al. [20]. The columns diameters of the multi-column piers of bridges with span length of 30 m were in the range of 0.9–1.8 m and in the range of 1.60–3.10 m for single-column piers. 5-m high bridges on low seismicity zones have the smallest column diameter and 20-m high bridges on high seismicity zones have the largest dimension. Steel ratios were in the range of 2.85–3.22% and 2.83–3.13% for multi-column and single-column piers, respectively. 50-m span bridges supported on multi-column piers had column diameters in the range of 0.95–1.85 m and diameters in the range of 1.70–3.20 m for single-column piers. In these cases, the steel ratios were in the range of 2.83–3.24% and 2.82–3.05%, respectively.

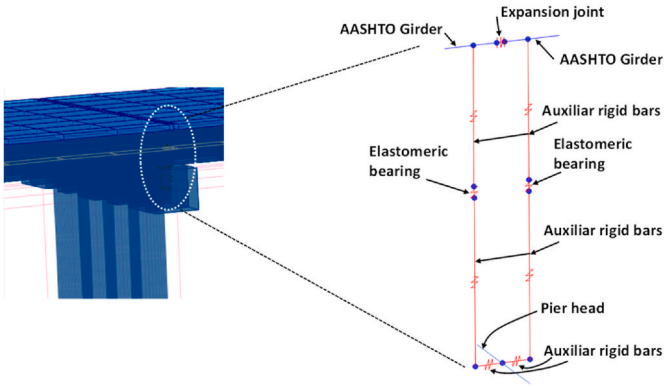

Fig. 5. Detail of the numerical model of expansion joint and elastomeric bearings.

The bridges were assumed to be on hard ground sites; therefore, the soil structure interaction (SSI) was neglected and fixed supports at base of columns were considered. Bridges on other type of soils should be designed incorporating the effects of SSI and subjected to accelerograms recorded in flexible ground sites. The overstrength of bridges on hard soils cannot be extrapolated to flexible soils because the effects of SSI in the seismic response of bridges can be beneficial or detrimental, as a function of the dynamic properties of the bridges, the frequency content of seismic records and the dynamic properties of the soils, among other variables [23,24].

Dynamic properties of the bridges and response spectra are important information to evaluate the results of nonlinear analyses. Fig. 6 provides a graphical representation of the bridges' fundamental periods in both directions of analysis. In the longitudinal direction the periods are in the range of 0.94–3.29 s for the bridges located in the LS zone; in the range of 0.89–2.94 s for the MS zone and in the range of 0.85–2.42 s for the HS zone. In the transverse direction, these intervals are 0.87–3.81 s, 0.85–2.82 s and 0.83–2.42 s for the three seismic zones, respectively.

The notation used to identify the bridges is as follows: M and C stands for multi-column or single-column piers, followed by the span length, the pier height and a number that identifies the bridge location as LS = 1 (low seismicity), MS = 2 (medium seismicity) and HS = 3 (high seismicity). Table 1 shows the results of the bridge design [20] using SAP2000 software [25]. It includes span length, pier height, bridge seismic location, column diameter, longitudinal steel ratio and the notation used to identify each numerical model.

4. Nonlinear analysis

4.1. Pushover analysis

The overstrength factors were computed with static and dynamic nonlinear analyses. Pushover analyses allowed determining the ultimate base shear and the ratio of this value to the design base shear defines the overstrength factor. Nonlinear models were created with the SAP2000 program [25] assigning plastic joints at both ends of each column and discretizing their cross sections with fibers. The cross section was divided into many integration points and each fiber was described with a uniaxial constitutive law (stress-strain). Confined concrete constitutive model was used for the fibers inside the concrete core, while the unconfined concrete constitutive model was adopted for the fibers out of the concrete core [26]. The constitutive model of Park and Paulay [27] defined the uniaxial behavior of the reinforcing steel. Thus, moment-rotation relationships describing the nonlinear behavior of plastic hinges, could be obtained using the constitutive models of the reinforcing steel and the confined and unconfined concrete. The length of plastic hinges was determined according to the proposal of Paulay and Priestley [28].

The fundamental mode defined the load shape pattern applied in pushover analysis (displacement control). The control node was on the bridge deck at the span center between piers 2 and 3. As an example of these results, Fig. 7 shows the pushover curves in both directions of the M30P10-3 bridge (Fig. 7b) and the rotation demands in each column of the four piers (Fig. 7c–j).

The bridge capacity in the transverse direction was greater than the capacity in the longitudinal direction. The rotation demands of the four columns in each pier of the longitudinal direction were similar, although rotation demands were higher in the intermediate piers. Conversely, in the transverse direction, in addition to present larger rotation demands in the intermediate piers, the four columns in each pier presented different rotation demands. This noticeable effect in the transverse direction of the piers is due to the frame-type behavior and to the variation of column axial loads during the seismic movement, particularly between extreme and central columns.

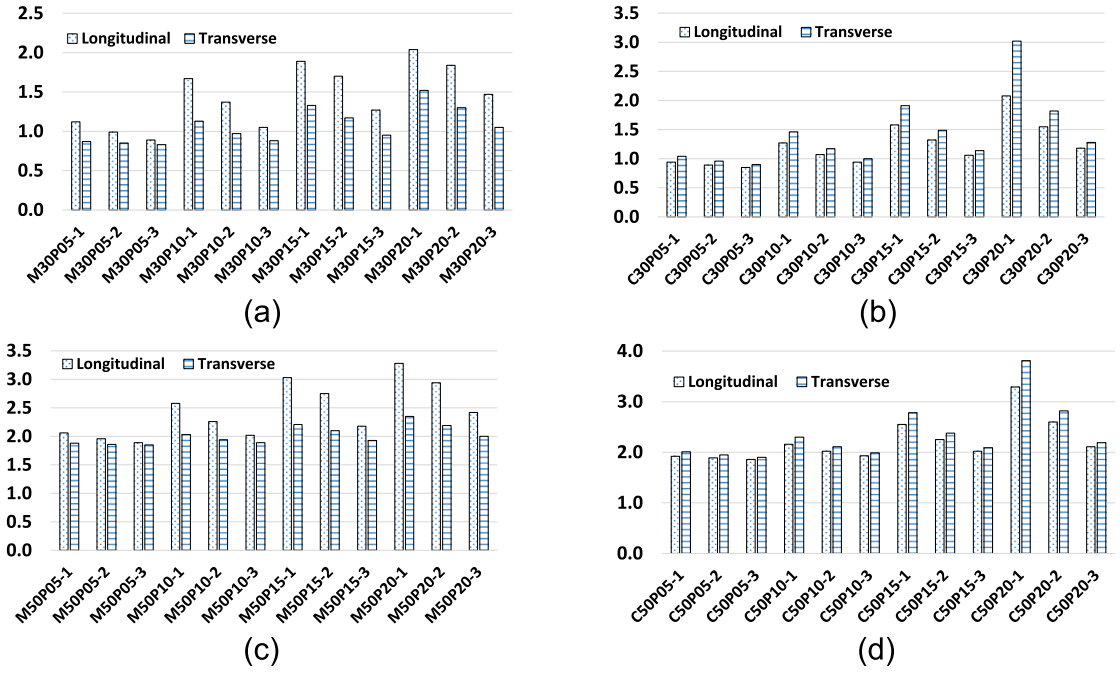

Fig. 6. Fundamental periods of the bridges. (a) 30 m span bridges with multi-column piers; (b) 30 m span bridges with single-column piers; (c) 50 m span bridges with multi-column piers and (d) 50 m span bridges with single-column piers.

Fig. 8 shows pushover analysis in both directions of the C30P10-3 bridge. This bridge with a substructure formed by single-column piers presented a very similar behavior in the longitudinal and the transverse direction; however, longitudinally the bridge capacity was slightly greater than transversely. In both directions, central piers had higher seismic rotation demands than the extreme piers. These results were consistent with the behavior observed in M30P10-3 bridge, where central piers had higher demands as well.

4.2. Dynamic analysis

To evaluate the effect of the seismic source and methodology used to assess the overstrength factors of the bridges, nonlinear dynamic analysis was performed assuming a damping ratio of 1%. The bridges were subjected to a set of 45 accelerograms of interplate earthquakes and 45 seismic records of intraplate source. As an example of these analyses, Fig. 9 shows base shear demands (V) vs. drift ratios (Δ/H) of pier 3 (M30P10-3 bridge), subjected to the CALE8509.191 seismic record.

Fig. 9a and b shows the bridge response in the longitudinal and transverse directions, respectively. Fig. 9 also displays the bridge capacity curves obtained with the pushover analysis. These results showed a good correlation with the hysteretic behavior obtained with the dynamic analysis. The longitudinal direction, with less stiffness than the transverse direction, presented larger displacement demands. The greater stiffness of the bridge in the transverse direction was evident in the slope of the load-deformation curve.

Similarly, Fig. 10 shows base shear demands vs drift ratios of a central pier (pier 3) of the C30P10-3 model subjected to the seismic record SJLL204.01213. Figs. 10a and b shows the seismic response in the longitudinal and transverse directions, respectively.

Unlike the previous case of multi-column piers, the seismic response of the bridges with a substructure formed by single-column piers showed similar behavior in both directions of analysis, whereas shear demands from dynamic analysis were still higher in the longitudinal direction of the bridge. An important difference between multi-column and single-column pier bridges was the base shear capacity in both directions of analysis. Single-column pier bridges presented similar base shear capacities in the longitudinal and transverse directions, whereas multi-column pier bridges showed notably higher base shear capacity in the transverse direction than that of the longitudinal direction.

The overstrength of the bridges was determined by subjecting the bridges to the set of seismic records scaled to reach the failure in the concrete or the reinforcing steel. Fig. 11 shows the stress-strain curve of one longitudinal reinforcement fiber (constitutive model of [27], located at the column plastic hinge of the M30P10-3 bridge model (10a) and C30P10-3 model (10b). Both diagrams also show the dynamic behavior of the selected fiber. The steel stress-strain backbone curve, from the elastic zone to the failure, satisfactorily encloses the stress-strain behavior obtained with the dynamic analysis.

5. Overstrength factors

The overstrength factors for the longitudinal and transverse directions of the bridges, subjected to the set of accelerograms from each seismic source were obtained. The ratio of the ultimate base shear to design base shear was determined with pushover analysis and nonlinear dynamic analysis. The ultimate base shear was the base shear demand when the bridge reached one of following failure mechanism: a collapse mechanism achieved in any of the piers or a local collapse in a plastic hinge attained when a tension strain demand in the longitudinal steel equal its maximum capacity or a compression strain in a concrete fiber reached its maximum capacity. The latter was determined with the moment-curvature relationships of each plastic hinge. As mentioned before, a significant number of published studies reports overstrength factors based exclusively on nonlinear static analysis. The following sections discuss the influence of the seismic source on the overstrength factors computed with nonlinear static analysis and nonlinear dynamic analysis.

5.1. Interplate earthquakes

5.1.1. Bridges with span length of 30 m

Fig. 12 shows the overstrength factors, in both directions of the 30 m span bridges with frame-type substructure (M30), obtained with

Table 1
Numerical model characteristics of the bridges (adapted from [20].

Model ID	Span length (m)	Pier height (m)	Bridge location	Column diameter (m)	Steel ratio (%)	Model ID	Span length (m)	Pier height (m)	Bridge location	Column diameter (m)	Steel ratio (%)
M30P05-1	30	5	LS	0.90	2.9	M50P05-1	50	5	LS	0.95	3.2
M30P05-2			MS	1.05	2.9	M50P05-2			MS	1.10	2.9
M30P05-3			HS	1.25	3.0	M50P05-3			HS	1.30	2.8
M30P10-1		10	LS	0.95	3.2	M50P10-1		10	LS	1.05	2.9
M30P10-2			MS	1.15	3.0	M50P10-2			MS	1.25	3.2
M30P10-3			HS	1.50	3.0	M50P10-3			HS	1.55	3.0
M30P15-1		15	LS	1.12	2.9	M50P15-1		15	LS	1.18	3.0
M30P15-2			MS	1.25	3.1	M50P15-2			MS	1.30	3.2
M30P15-3			HS	1.65	3.1	M50P15-3			HS	1.75	3.0
M30P20-1		20	LS	1.30	2.9	M50P20-1		20	LS	1.35	2.9
M30P20-2			MS	1.45	2.9	M50P20-2			MS	1.50	2.9
M30P20-3			HS	1.80	2.9	M50P20-3			HS	1.85	3.0
C30P05-1	30	5	LS	1.60	2.8	C50P05-1	50	5	LS	1.70	2.9
C30P05-2			MS	1.80	2.8	C50P05-2			MS	1.90	2.8
C30P05-3			HS	2.05	3.1	C50P05-3			HS	2.20	2.9
C30P10-1		10	LS	1.75	3.1	C50P10-1		10	LS	1.90	3.0
C30P10-2			MS	2.10	2.8	C50P10-2			MS	2.20	2.8
C30P10-3			HS	2.50	3.0	C50P10-3			HS	2.55	3.0
C30P15-1		15	LS	1.90	2.9	C50P15-1		15	LS	2.00	2.9
C30P15-2			MS	2.25	3.0	C50P15-2			MS	2.35	3.0
C30P15-3			HS	2.80	3.1	C50P15-3			HS	2.90	2.9
C30P20-1		20	LS	1.75	3.0	C50P20-1		20	LS	1.90	2.8
C30P20-2			MS	2.40	3.1	C50P20-2			MS	2.40	3.1
C30P20-3			HS	3.10	3.0	C50P20-3			HS	3.20	2.8

pushover (PO) and dynamic (DYN) analyses of the bridges located in the zones of low (LS), medium (MS) and high seismicity (HS). The bridges were subjected to the set of accelerograms recorded in interplate earthquakes. Fig. 12a presents the overstrength factors in the longitudinal direction and Fig. 12b in the transverse direction. The horizontal axis displays three rows for the low, medium and high seismicity, and each row has the results of the pushover analysis (PO) and nonlinear dynamic analysis (DYN) for pier heights in the range of 5–20 m. The vertical axis shows the overstrength factor.

In the longitudinal direction, the pier height was found to have small influence on the overstrength factors of the bridges located in the highest seismic zone (HS). In this case, the overstrength factors varied in the ranges of 1.9–2.0 and 2.1–2.5 for the pushover and dynamic analyses, respectively. On the contrary, the overstrength factors showed a clear dependence on the pier height in the medium and low seismic zones; the higher the pier, the greater the overstrength factor. In the zone of medium seismicity, the factors were in the ranges of 2.3–5.2 and 2.4–5.2 for the pushover and dynamic analyses. In the low seismic zone, these intervals were in the range of 2.8–8.6 and 2.7–7.7. Higher bridges showed important differences in overstrength factors when going from zones of low to high seismicity, and the low seismic zone presented the greatest differences in the overstrength factors computed with nonlinear static and dynamic analyses.

In most cases, pushover analyses overestimate the overstrength factors, particularly in the bridges located in low seismicity areas. Pushover analyses overestimate the bridges overstrength because this methodology applies a monotonic load in each horizontal direction of the bridges independently. In the nonlinear dynamic analyses, the three orthogonal components of the seismic records (two horizontal and one vertical) were applied simultaneously. When ground accelerations act simultaneously in two horizontal and one vertical directions, the fiber strains in columns reach the failure limit state faster and, therefore, lower overstrength factors were obtained.

In the transverse direction (Fig. 12b), the increase of pier height reduced the overstrength factor and the maximum values were lower than those obtained in the longitudinal direction. The overstrength factors of the bridges located in the high seismic zone were in the range of 2.7–6.0 and 2.4–4.6, for the pushover analysis and the dynamic analysis, respectively. These ranges were 2.5–6.0 and 2.0–4.4 for the medium seismic zone and 2.9–5.9 and 2.5–5.0 for low seismic zone. The

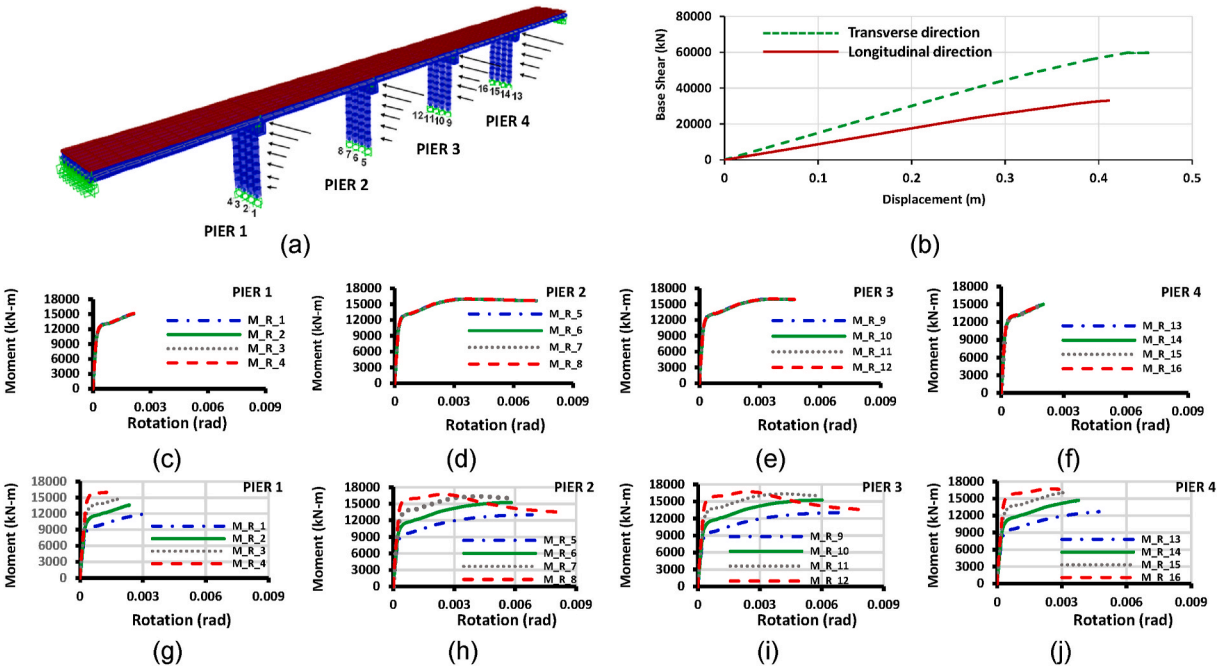

Fig. 7. Pushover analyses and moment-rotation demands in M30P10-3 model. (a) Bridge model indicating the direction of the transverse pushover analysis; (b) pushover analyses; (c-f) moment rotation curves of piers 1–4 in the longitudinal direction and (g-j) moment rotation curves of piers 1–4 in the transverse direction.

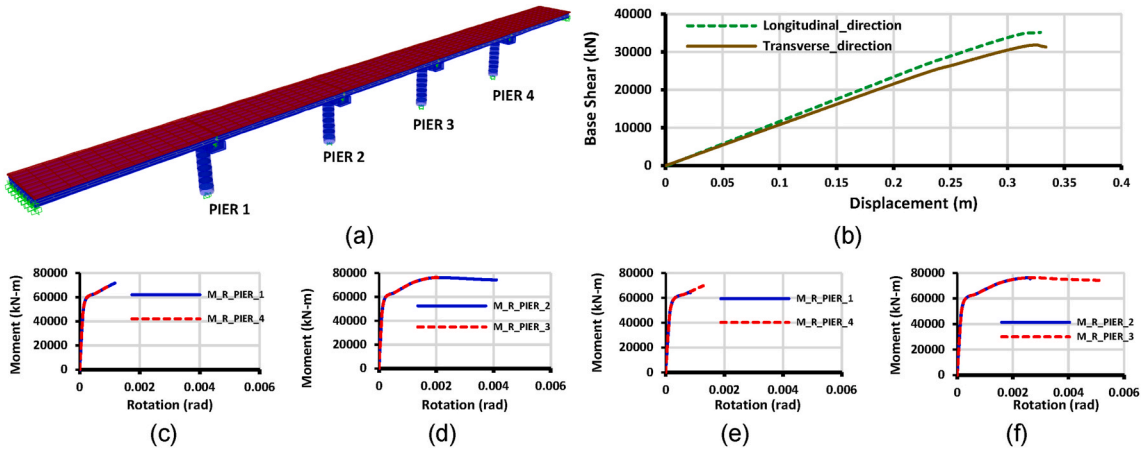

Fig. 8. Pushover analyses and moment-rotation demands in C30P10-3 model. (a) Bridge model; (b) pushover analyses; (c-d) moment rotation curves of piers 1–4 and 2–3 in the longitudinal direction and (e-f) moment rotation curves of piers 1–4 and 2–3 in the transverse direction.

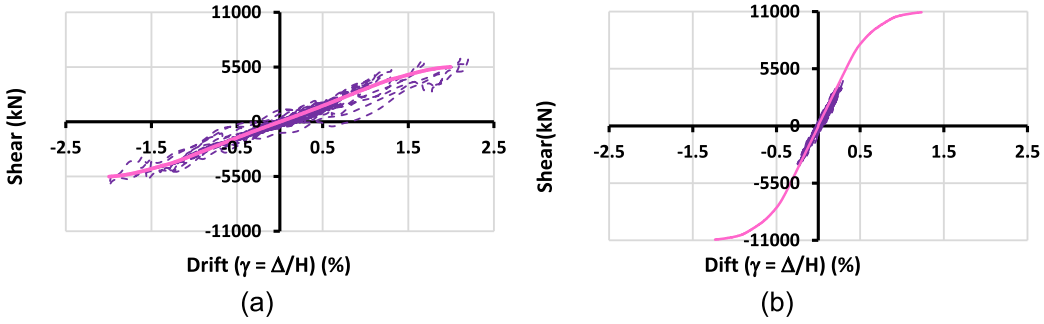

Fig. 9. Pushover analysis and dynamic response of M30P10-3 bridge (pier 3) subjected to CALE8509.191 seismic record. (a) Longitudinal direction and (b) transverse direction.

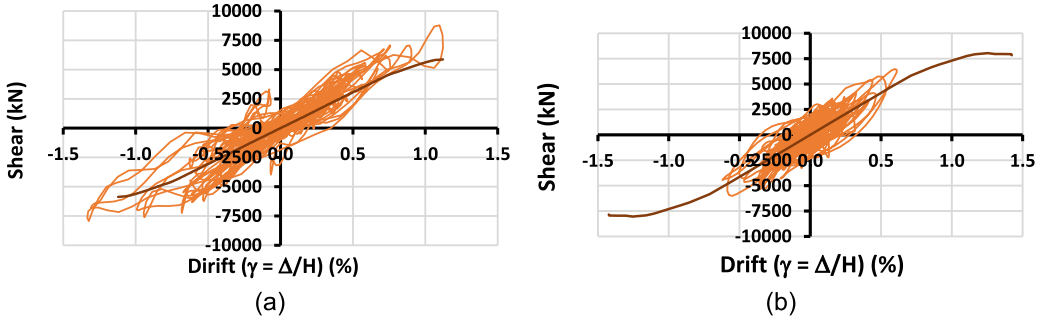

Fig. 10. Pushover analysis and dynamic response of C30P10-3 bridge subjected to SJLL204.01213 seismic record. (a) Longitudinal direction and (b) transverse direction.

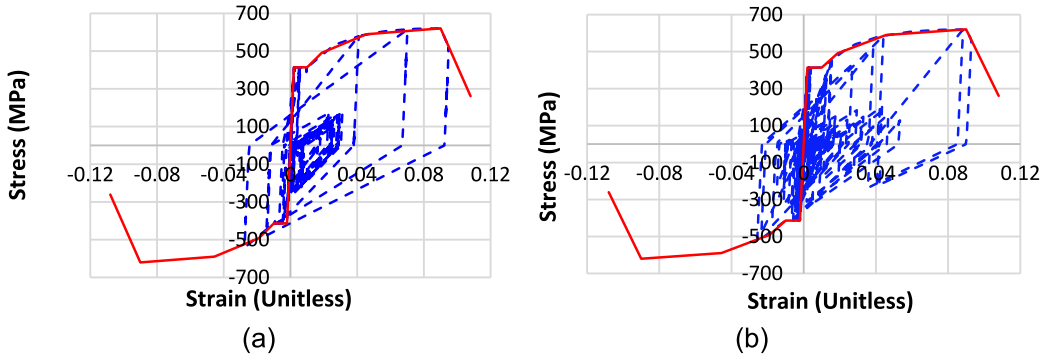

Fig. 11. Stress-strain response of a longitudinal reinforcement fiber and Park and Paulay constitutive model. (a) M30P10-3 bridge and (b) C30P10-3 bridge.

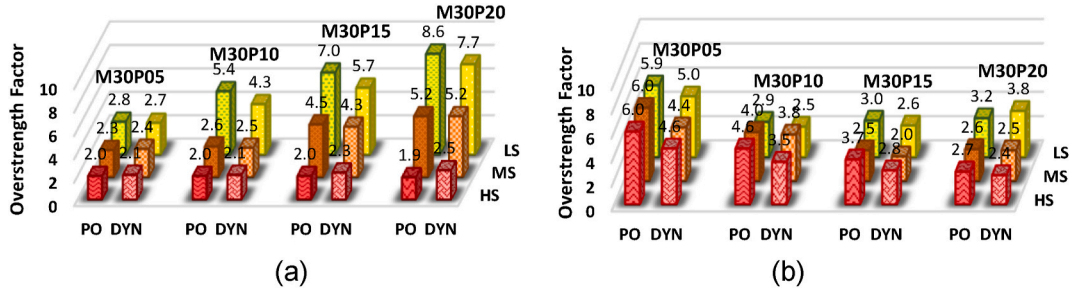

Fig. 12. Overstrength factors of multi-column piers 30 m span bridges. (a) Longitudinal direction and (b) transverse direction.

differences among the overstrength factors obtained with the two methodologies were more notable in this direction, particularly in the lower height bridges.

In the longitudinal direction, an increase in pier height led to a rise in the overstrength factor in the low and medium seismic zones. As the bridge height grows, there is an increase of displacement demands generating an important contribution of the soil-abutment in the overstrength factors. When moving from low to high seismicity zones, the trend of overstrength factors is different mainly because the design actions in low and medium seismicity zones have moderate participation of seismic loads and high contribution of gravity loads that increase overstrength factors. The seismic loads of the bridges on the high seismicity zone had the most important contribution in the design actions for all bridge heights, producing in this case similar overstrength factors.

In the transverse direction, frame-type piers formed by four columns and a cap beam support the bridge. The increase of the pier height reduced the overstrength factor; Jain and Navin [13]; and Mehanny and ElHoeary [15] in multi-story framed structures, reported similar results. In the high seismic zone, the increase of the pier height always reduced the overstrength factor. However, in the two remaining seismic zones, initially the overstrength factor decreased with the increase of pier height and subsequently grew slightly.

Fig. 13 shows the results for bridges with span of 30 m supported by single-column piers. Fig. 13a shows the overstrength factors for the longitudinal direction and Fig. 13b for the transverse direction.

Analogous to bridges formed by frame-type piers, in the longitudinal direction the overstrength factor increased with the increase in the pier height, although the increase rate was lower. This behavior showed that overstrength grows with structural redundancy. In the high seismic zone, both substructure types produced overstrength factors practically independent of the pier height, and both methodologies of analysis led to similar results. In this direction of analysis, the overstrength factors obtained with the pushover analysis were in the range of 2.7–3.1, 3.4–4.2 and 4.1–6.4, for the high, medium and low seismic zones, respectively, whereas dynamic analysis led to overstrength factors in the range of 2.7–3.1, 2.9–4.5 and 3.9–4.7, for the three seismic zones.

The transverse direction of the bridges with single-column piers displayed similar trends of overstrength factors observed in bridges

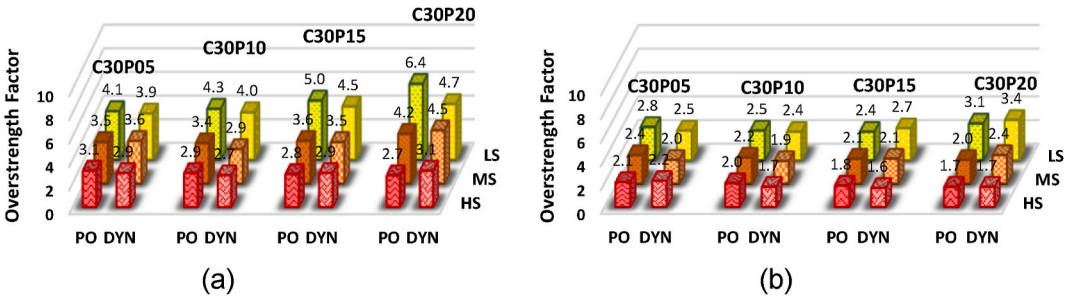

Fig. 13. Overstrength factors of single-column 30 m span bridges. (a) Longitudinal direction and (b) transverse direction.

supported by multi-column piers, although the overstrength factors were lower. In this case, the overstrength factors obtained with pushover analysis were in the range of 1.7–2.1, 2.0–2.4 and 2.4–3.1 for the high, medium and low seismic zones, respectively, and dynamic analysis produced overstrength factors in the range of 1.6–2.2, 1.9–2.4 and 2.4–3.4. Clearly, both types of analysis led to similar overstrength factors.

5.1.2. Bridges with span length of 50 m

Fig. 14 shows the overstrength factors in both directions of the 50 m span bridges supported by multi-column piers, subjected to the set of accelerograms recorded in interplate earthquakes. In general, overstrength factors presented similar trend in both directions of the 30 m span bridges. In the longitudinal direction, the increase of pier height led to a rise in overstrength factors, whereas in the transverse direction, overstrength factors decreased with the pier height increase. Both methodologies of analysis yielded to differences in overstrength factors like those differences obtained in the analysis of 30 m span bridges.

In the longitudinal direction, pushover and dynamic analyses led to overstrength factors in the range of 1.7–7.4 and 1.8–8.4, respectively. These intervals were similar to those obtained in the analysis of 30 m span bridges (1.9–8.6 and 2.1–7.7). In the transverse direction, pushover analysis led to overstrength factors in the range of 1.8–6.2 and 1.6–4.6 for the 50 m and 30 m span bridges, respectively, whereas dynamic analysis produced overstrength factors in the range of 1.6–4.6 and 2.0–5.0 for both span lengths.

Fig. 15 shows the overstrength factors of the 50 m span bridges supported by single-column piers. Although the overstrength factors were slightly lower than those obtained for the 30 m span bridges, the trends observed in both directions of the bridges were similar. In the longitudinal direction, the overstrength factors were in the range of 2.5–5.4 with pushover analysis (2.7–6.4 for the 30 m span bridges). Dynamic analysis led to overstrength factors in the range of 1.4–3.1 and 1.6–3.4 for 50 m and 30 m span bridges, respectively. Again, pushover analysis overestimates the overstrength factors.

5.2. Intraplate earthquakes

5.2.1. Bridges with span length of 30 m

Fig. 16 shows the overstrength factors for the 30 m span bridges supported by multi-column piers (M30) and single-column piers (C30). The dynamic analysis of the bridges subjected to the set of accelerograms recorded in intraplate earthquakes reduced, in general, the overstrength factors obtained with the seismic records of subduction earthquakes. This behavior shows the influence of the frequency contents of the seismic movements, parameters not included in pushover analysis. The accelerograms recorded from intraplate earthquakes presented larger spectral amplitudes for the bridges' fundamental periods than those of the subduction records.

Although the overstrength factors of the bridges subjected to intraplate earthquakes were smaller, the trend, as a function of the pier height and seismicity level, is similar for both seismic sources. Pushover analysis overestimates overstrength factors, particularly in bridges supported by multi-column piers. The effect is more noticeable because the seismic component in the transverse direction of multi-column bridges had greater participation in the seismic response of the bridges than its participation in single-column bridges. The above is explained by observing the fundamental periods in the longitudinal and transverse directions of the bridges with both substructure types and the response spectra of Fig. 2; whereas the fundamental period in the transverse direction of the multi-column bridges is reduced with respect to their fundamental period in the longitudinal direction, leading the bridge to spectral zones of higher amplitude, the opposite occurs in single-column bridges. The greater participation of the transverse seismic component in multi-column bridges makes the difference between pushover analyses and dynamic analyses more evident.

5.2.2. Bridges with span length of 50 m

Fig. 17 shows the overstrength factors for the bridges with span length of 50 m subjected to accelerograms recorded in intraplate earthquakes. Again, this set of ground motions reduced the overstrength factors obtained with the analysis of the bridges subjected to seismic records produced in interplate faults. The influence of pier heights and seismic zones on overstrength factors was similar for both groups of seismic records.

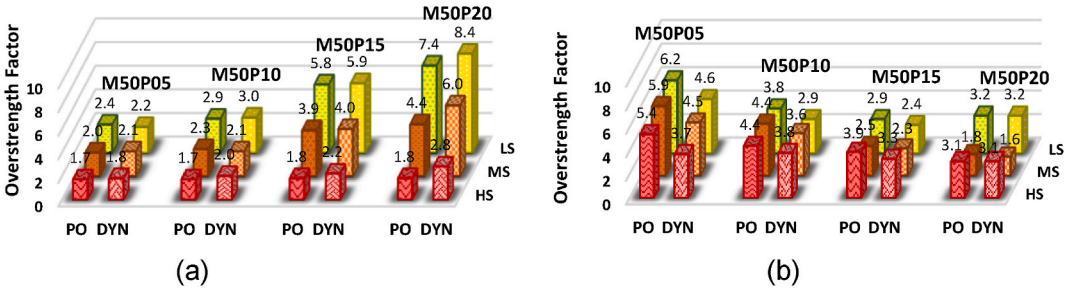

Fig. 14. Overstrength factors of multi-column 50 m span bridges. (a) Longitudinal direction and (b) transverse direction.

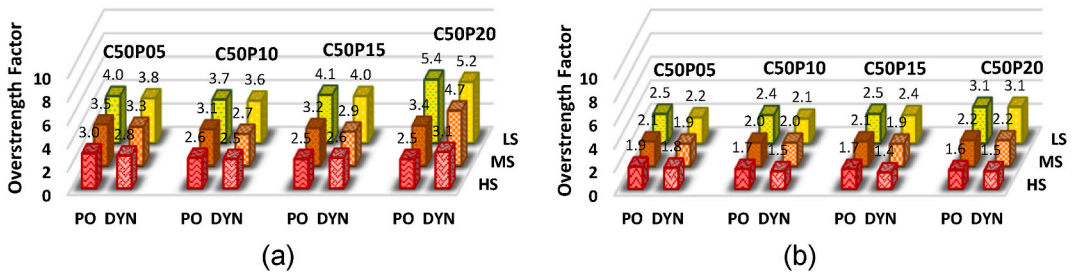

Fig. 15. Overstrength factors of single-column 50 m span bridges. (a) Longitudinal direction and (b) transverse direction.

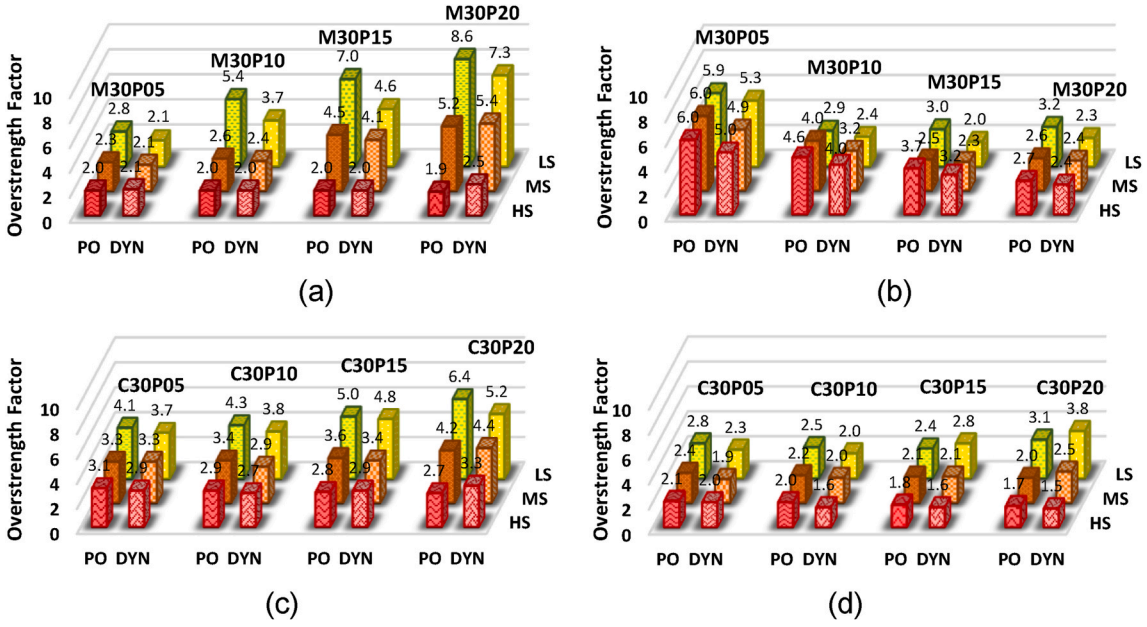

Fig. 16. Overstrength factors of the 30 m span bridges subjected to accelerograms originated in intraplate faults. (a) M30 bridges in the longitudinal direction; (b) M30 bridges in the transverse direction; (c) C30 bridges in the longitudinal direction and (d) C30 bridges in the transverse direction.

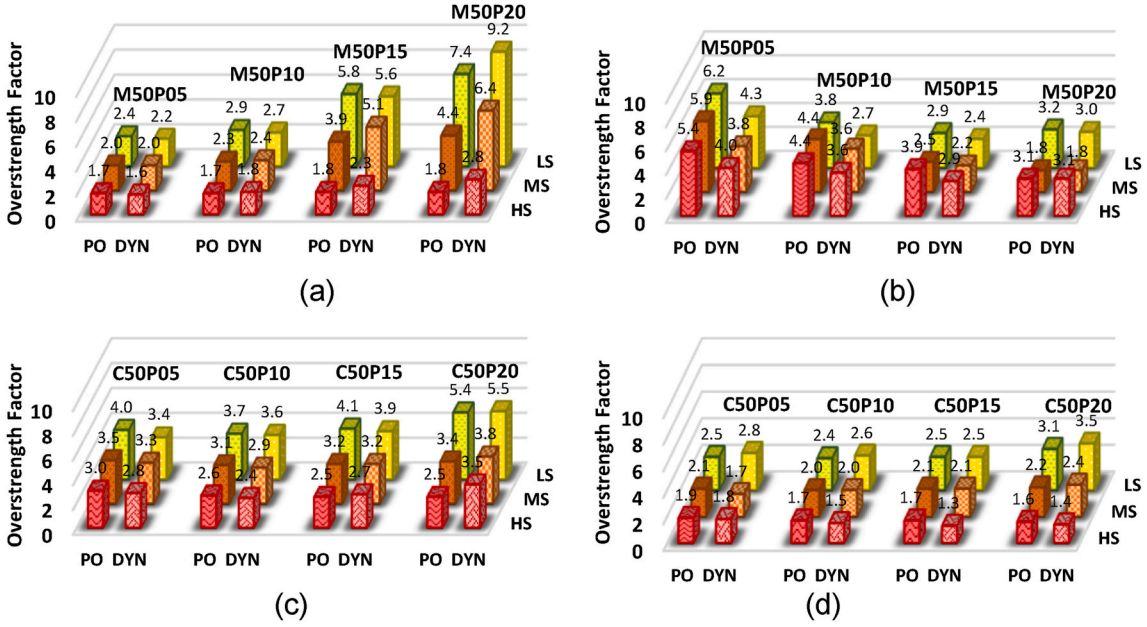

Fig. 17. Overstrength factors of the 50 m span bridges subjected to accelerograms originated in intraplate faults. (a) M50 bridges in the longitudinal direction; (b) M50 bridges in the transverse direction; (c) C50 bridges in the longitudinal direction and (d) C50 bridges in the transverse direction.

Despite that in general terms the pushover analyses continue to overestimate the overstrength factors, the differences between the overstrength obtained with the nonlinear static analysis and the dynamic analysis in the 50 m span bridges, were slightly smaller.

5.3. Capacity curves

For a better understanding of the trend observed in overstrength factors obtained in the previous section for each seismic zone, the following figures show the design base shear and the shear seismic capacity of the M30P05 and M30P20 bridges, calculated with pushover analysis in the longitudinal and the transverse directions. Fig. 18 shows base shear force (vertical axis) vs lateral displacement of the bridge (horizontal axis) in the longitudinal direction. Moving the bridge location from the high to low seismicity zone accentuated the difference between the overstrength factors of the 5 m and 20 m high bridges. While the ratio of ultimate base shear (V_{uL}) to design base shear (V_{dL}) in the three seismic zones, was similar for the 5 m high bridges, this ratio was strongly dependent on the seismic zone for the 20 m high bridges. The design base shear in 20 m high bridges grows in greater proportion than the ultimate base shear, when moving from low to high seismicity zones, which justifies the observed behavior in overstrength factors. Fig. 16 also shows the overstrength factors for the 5 m high bridge, q_{sL} (H = 5 m), and for the 20 m high bridge, q_{sL} (H = 20 m).

Fig. 19 shows the design and ultimate base shear in the transverse direction of the M30P05 and M30P20 bridges. In this direction, the overstrength factors had a different trend than that observed in the longitudinal direction. When moving the bridge location from the low seismic zone to the high seismic zone, the overstrength increases. The frame-type behavior in this direction produced a significant increase of the ultimate base shear of the bridges located in the zone of low seismicity to the bridges located in the zone of high seismicity [13]. and Mehanny and El Howary [15] had previously reported this trend of behavior.

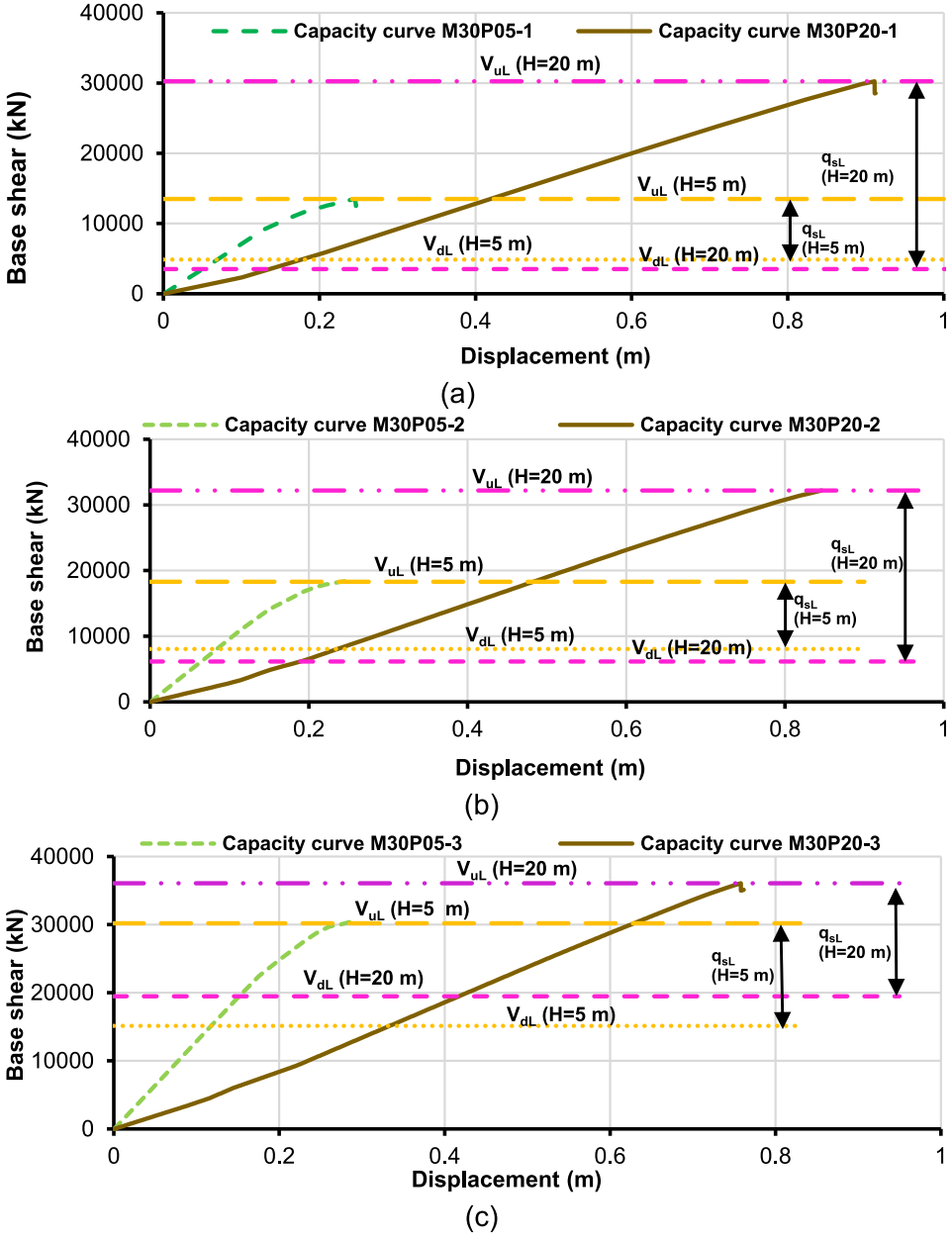

Fig. 18. Capacity curves in the longitudinal direction of the M30P05 and M30P20 bridges. (a) Low seismic zone; (b) medium seismic zone and (c) high seismic zone.

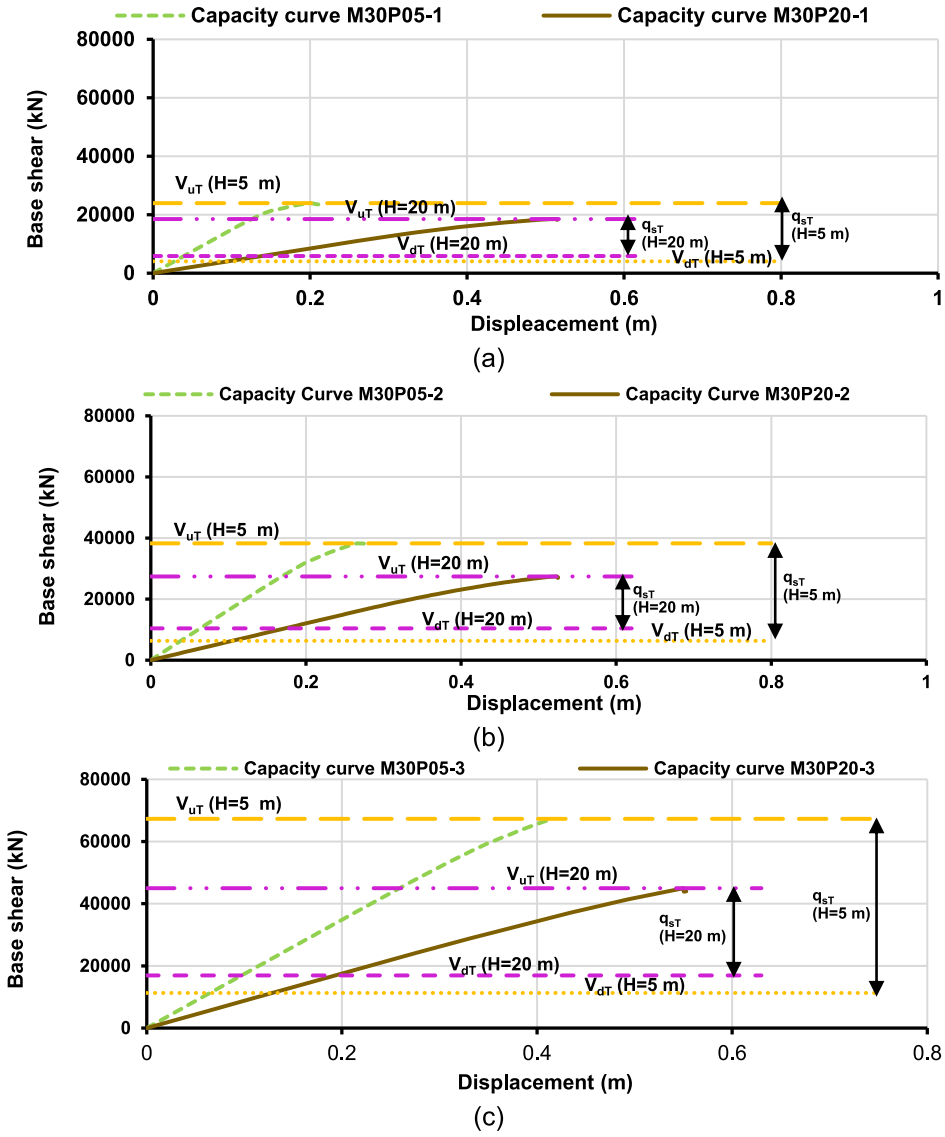

Fig. 19. Capacity curves in the transverse direction of the M30P05 and M30P20 bridges. (a) Low seismicity zone; (b) medium seismicity zone and (c) high seismicity zone.

5.4. Influence of the bridge location and seismic source

Fig. 20 shows the overstrength factors of the 30 m span bridges supported by multi-column and single-column piers. Figs. 20a and b displays the overstrength factors of the M30 bridges in the longitudinal and the transverse directions, respectively. Similarly, Figs. 20c and d presents the results of the C30 bridges in both directions of analysis. Each diagram shows six curves for the three bridge locations and the three seismic zones. S stands for subduction earthquakes (interplate), N stands for normal fault earthquakes (intraplate), while HS, MS and LS display the results for bridges located in high, medium and low seismic zones, respectively.

The overstrength factors in the longitudinal direction of the bridges located in zones of medium and high seismicity, presented very similar values for the two groups of seismic records. However, in the low seismicity zone, the differences between the two seismic sources were more significant, particularly in bridges supported on multi-column piers.

Again, in the transverse direction, the low seismicity zone showed that overstrength factors were clearly dependent on the seismic source. E.g., the 20 m high bridge supported by frame-type piers, located in the low seismic zone, displayed overstrength factors in the range of 2.3–3.8, as a function of the seismic source of the ground motions.

Fig. 21 shows the overstrength factors of the 50 m long bridges. Apart from the bridges in the medium seismic zone, the overstrength factors in the longitudinal direction were entirely similar for the two groups of seismic sources. The most important impacts of the seismic source on overstrength factors of the bridges located in the medium seismicity zone were for 15-m and 20-m high bridges. The 15 m high bridges supported by multi-column piers had overstrength factors of 4.0 and 5.1 for interplate and intraplate faults, respectively, and the 20 m high bridge supported by single-column piers presented overstrength factors of 4.7 and 3.8 when subjected to the set of interplate and intraplate accelerograms.

Unlike the 30 m span bridges, in the transverse direction of the 50 m span bridges, the overstrength factors obtained with the accelerograms of the two seismic sources are closer to each other when the substructures are composed by multi-column piers. The 50 m span bridges formed with single-column piers in low seismicity zone presented the greatest difference in the overstrength factors: 2.2 for interplate events and 2.8 for intraplate events.

Previous results showed that the overstrength factors of medium-length bridges depended on the seismic source, piers height, seismic

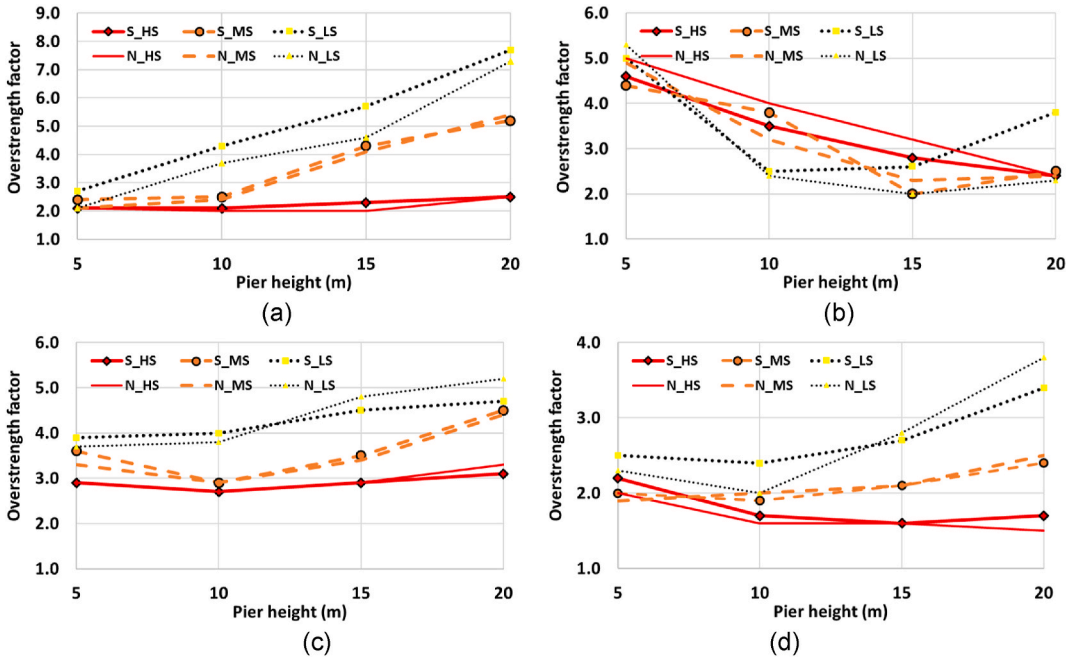

Fig. 20. Overstrength factors of the 30 m span bridges subjected to interplate (S) and intraplate (N) seismic records. (a) Longitudinal direction of M30 bridges; (b) transverse direction of M30 bridges; (c) longitudinal direction of C30 bridges and (d) transverse direction of C30 bridges.

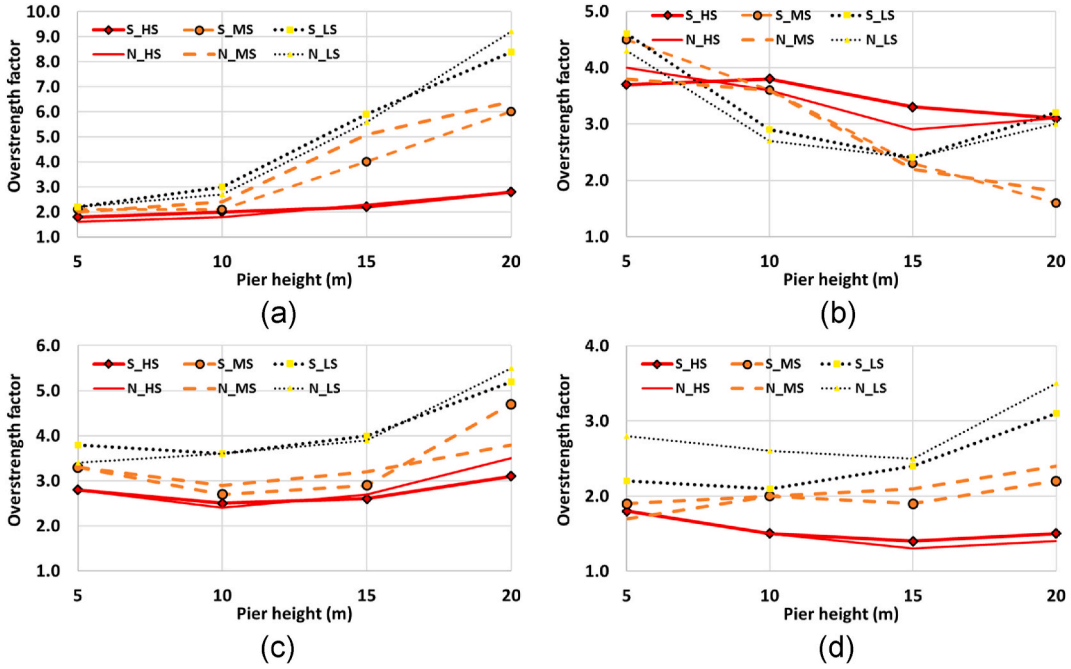

Fig. 21. Overstrength factors of the 50 m span bridges subjected to interplate (S) and intraplate (N) seismic records. (a) Longitudinal direction of M50 bridges; (b) transverse direction of M50 bridges; (c) longitudinal direction of C50 bridges and (d) transverse direction of C50 bridges.

location of the structures and the direction of analysis. Other authors (Jain and Navin, 1995 [14,15,17]; found similar results. The bridges located in zones of low seismicity showed more dependency on the seismic source that could justify the use of two different expressions to obtain the overstrength factors, as a function of the seismic source with more contribution in the site seismic hazard.

5.5. Comparison of overstrength equations

Based on the previous results, a polynomial regression was performed to propose equations for the overstrength factors as a function of the variable T (H/L), for each group of seismic records (interplate and intraplate sources) and for each substructure type (multi-column and single-column piers). T is the fundamental period of the bridge in the direction of analysis, H is the pier height, and L is the span length. To show the influence of the seismic source on the overstrength factors, Fig. 22 presents six diagrams corresponding to the equations obtained for each seismic source and seismic location of the multi-column bridges. Fig. 22 also shows overstrength factors obtained in the study of Sánchez et al. [20]; where a set of accelerograms from various seismic

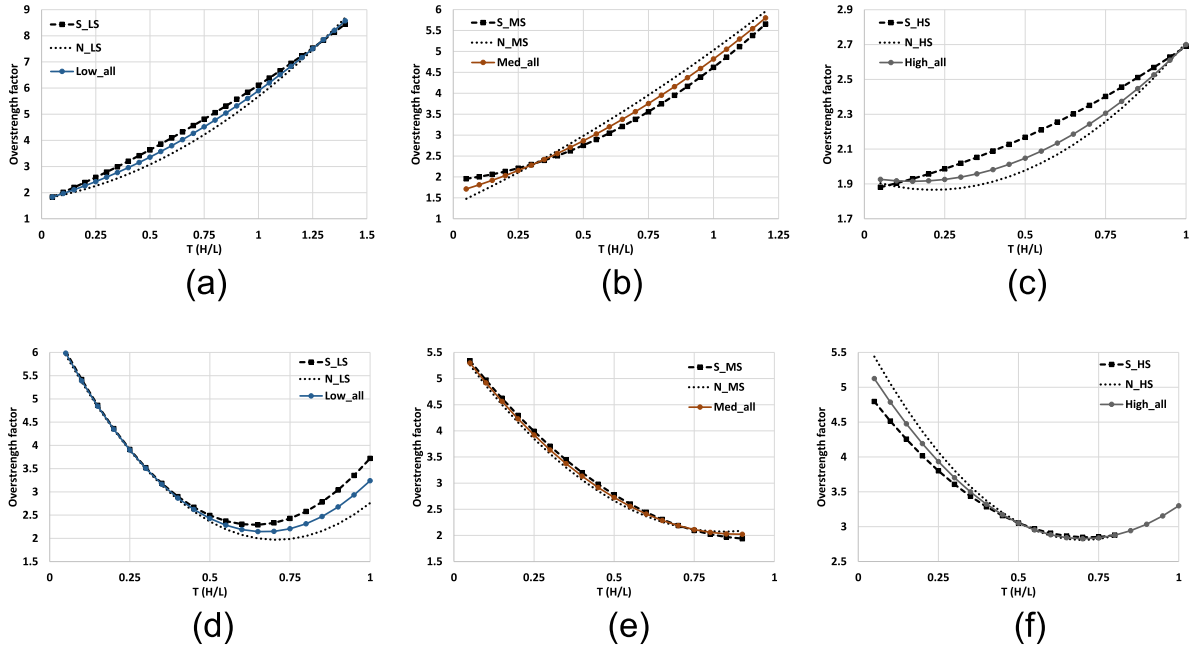

Fig. 22. Comparison of overstrength functions for multi-column bridges obtained with accelerograms from interplate earthquakes (S), intraplate earthquakes (N) and seismic records collected from more than one seismic source (all). Longitudinal direction (a-c) and transverse direction (d-f).

sources was used to assess overstrength factors. The curves follow the notation: X_LS, X_MS and X_HS, where X is the seismic source, namely S (interplate earthquakes) and N (normal fault, intraplate earthquakes), and LS, MS and HS stand for low seismicity, medium seismicity and high seismicity, respectively. The equations proposed in the study of Sánchez et al. [20]; are identified as Low_all, Med_all and High_all for the three seismic locations of the bridges. The diagrams (a-c) present the longitudinal direction of the bridges and the diagrams (d-f) display the transverse direction.

To evaluate the overestimation or underestimation of the overstrength factors, it was determined the ratio of the overstrength factors obtained for each seismic source (S = subduction; N = Normal) to overstrength factors attained when using the equations based on the suite of accelerograms from various sources (All), for each T (H/L) value. Table 2 shows the maximum and minimum values of the overstrength ratios. Values above 1, indicate that combining seismic records from various sources leads to underestimated overstrength factors, whereas ratios below 1 imply the opposite (overestimation).

The overstrength underestimation can be up to 15% in the transverse direction of bridges supported in multi-column piers, located in areas of low seismicity, and the overestimation can reach up to 17% (inverse of 0.85). If a value of 10% is considered as an acceptable limit of the overstrength underestimation or overestimation, it is suggested to use an individual equation to calculate the overstrength factors for each seismic source in the cases shown in Table 3. These cases are: a) longitudinal direction of bridges supported on multi-column piers, located in a zone of medium seismicity and b) transverse direction of bridges supported on multi-column piers, located in a zone of low seismicity. The use of one or the other equation would depend on the seismic source that most contributes to the seismic hazard at the site of the bridge location. In the other cases, the equations proposed in Sánchez et al. [20]; which do not make any distinction from the seismic source, could be used. The coefficient of determination R^2 was in the range of 0.86–0.94.

The equations in Table 3 lead to overstrength factors of the bridges in the range of 1.6–6.9. Other authors reported in RC buildings overstrength factors in the range of 2.0–7.7 [10,11,14]. Kappos et al. [17] report overstrength factors for bridges in the range of 1.2–5.8. The force-reduction factors R that include ductility and overstrength in the AASHTO code [29] for single-column piers are in the range of 1.50–3.0 and for multi-column piers are in the range of 1.50–5.0. In AASHTO approach, the overstrength is the minimum possible value because it is assumed an elasto-plastic behavior without including the strain

Table 2
Maximum and minimum overstrength ratios. Seismic records from single seismic source (S, N)/combinations of seismic records from more than one seismic source (All).

Type of Pier	Direction	Seismicity	Ratio (S or N/All)			
Multi-column			$(S/All)_{max}$	$(S/All)_{min}$	$(N/All)_{max}$	$(N/All)_{min}$
	Longitudinal	Low	1.08	0.99	1.01	0.92
		Medium	1.14	0.95	1.05	0.86
		High	1.06	0.98	1.00	0.97
	Transverse	Low	1.15	1.00	1.00	0.85
		Medium	1.02	0.96	1.03	0.98
		High	1.01	0.94	1.06	0.99
Single-column	Longitudinal	Low	1.05	0.96	1.04	0.95
		Medium	1.06	0.97	1.03	0.94
		High	1.01	0.98	1.04	0.99
	Transverse	Low	0.98	0.94	1.07	1.03
		Medium	1.06	0.96	1.03	0.94
		High	1.09	1.00	0.99	0.94

Table 3
Equations to evaluate overstrength factors for 30 m and 50 m span bridges.

Bridge pier	Direction	Seismic intensity zone	Seismic fault	Overstrength function	R^2
Multi-column	L	Medium	S	$q_s = 2.06(\frac{TH}{L})^2 + 0.64(\frac{TH}{L}) + 1.92$	0.93
			N	$q_s = 0.79(\frac{TH}{L})^2 + 2.91(\frac{TH}{L}) + 1.33$	0.91
	T	Low	S	$q_s = 10.85(\frac{TH}{L})^2 - 13.82(\frac{TH}{L}) + 6.69$	0.94
			N	$q_s = 9.21(\frac{TH}{L})^2 - 13.02(\frac{TH}{L}) + 6.57$	0.86

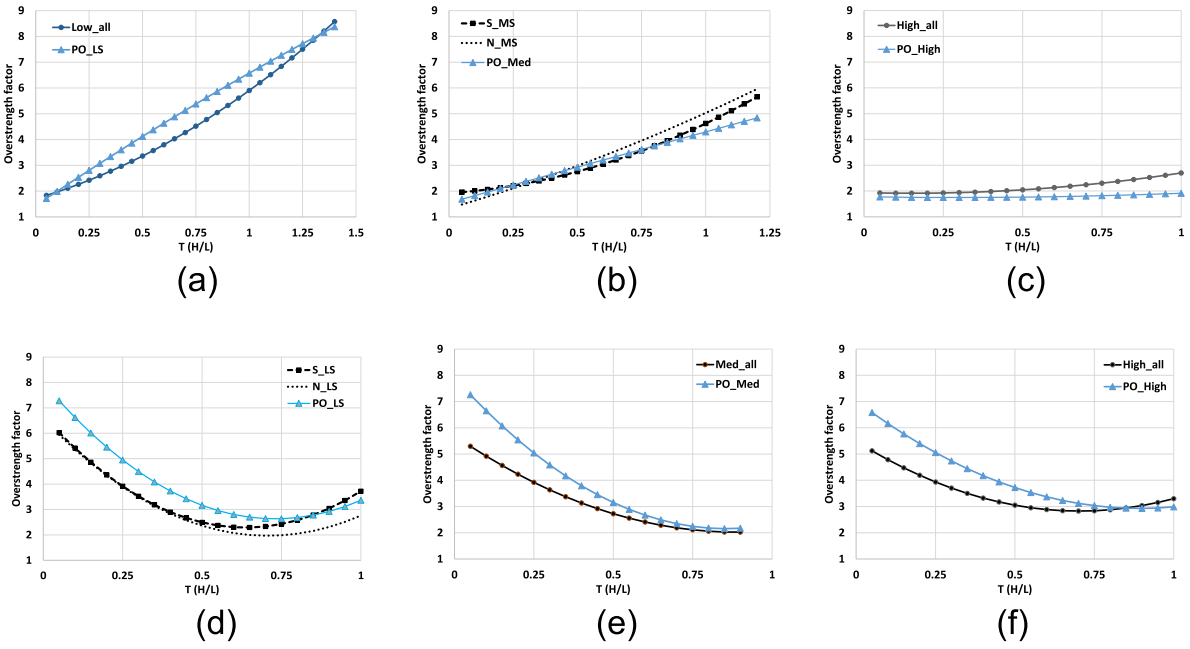

Fig. 23. Comparison of overstrength functions for multi-column bridges obtained with dynamic (S, N, or all) and pushover analyses (PO). Longitudinal direction (a-c) and transverse direction (d-f).

hardening region.

To evaluate the applicability of pushover analysis to assess overstrength factors, Fig. 23 shows a comparison of the overstrength factors obtained with the proposed equations (based on dynamic analyses) and those calculated with the non-linear static analyses for the bridges supported in multi-column piers. Whereas the seismic source showed a marginal influence in most of the cases analyzed, using a more refined methodology (non-linear dynamic analysis) appreciably modifies the results obtained with the pushover analysis. Although nonlinear static analyses may underestimate or overestimate the overstrength, in most cases the overstrength factors are overestimated, in relation to those calculated with dynamic analyses. Some diagrams show only two curves (one for dynamic analysis and other for pushover analysis) and the others have three curves (two for dynamic analysis of each seismic source and one for pushover analysis), in the cases where different overstrength functions are proposed for each seismic source.

Table 4 shows the maximum and minimum values of the overstrength ratios (dynamic analysis/static analysis). Again, values above 1 indicate that using the equation obtained with pushover analysis underestimates the overstrength factors and values below 1 overestimate the bridge overstrength. In the cases with two equations, as a function of the seismic source with the greatest contribution to the seismic hazard,

Table 4
Maximum and minimum overstrength ratios. Overstrength factors from dynamic analysis/overstrength factors from static analysis.

Type of Pier	Direction	Seismicity	Eq.	Overstrength ratio (S,N, or All/PO)			
Multi-column				$(S/PO)_{max}$	$(N/PO)_{max}$	$(S/PO)_{min}$	$(N/PO)_{min}$
	Long	Low	All	1.07		0.82	
		Medium	S,N	1.17	1.23	0.94	0.88
		High	All	1.41		1.09	
	Trans	Low	S,N	1.11	0.82	0.78	0.74
		Medium	All	0.94		0.73	
		High	All	1.10		0.78	
Single-column	Long	Low	All	0.96		0.85	
		Medium	All	1.10		0.90	
		High	All	1.24		0.93	
	Trans	Low	All	1.16		0.97	
		Medium	All	1.11		0.77	
		High	All	1.05		0.84	

two overstrength ratios are presented.

Overstrength factors can be underestimated by up to 41% when using pushover analysis, (longitudinal direction of multi-column piers, in a zone of high seismicity) and overestimated by up to 37% (transverse direction of multi-column piers, in a zone of medium seismicity). In accordance with the previous results, the selection of the seismic records to perform the dynamic analyses had less impact than the methodology used (static or dynamic) to obtain the overstrength factors. Clearly, pushover analyses overestimate most of the cases the overstrength factors.

6. Conclusions

This study evaluated the effect of the seismic record selection from two seismic sources, with independent occurrence processes that are capable of generating large earthquakes, on the overstrength factors of medium-length reinforced concrete bridges. It was also analyzed the impact of the methodology used (nonlinear static analysis vs nonlinear dynamic analysis) on the bridges overstrength. The analysis included two span lengths (30 m and 50 m) and two types of substructures: multi-column piers and single-column piers. The results allowed evaluating overstrength factors for this type of bridges as a function of the seismic source, seismic location of the bridge (low, medium and high seismicity), substructure type, direction of analysis and the applied methodology. The results led to the conclusions described next.

Although there are important differences on the seismological processes of interplate and intraplate earthquakes, the general trend of the overstrength factors of the bridges as a function of the parameters included, was similar in most of the cases. However, the overstrength factors of multi-column bridges located in low and moderate seismic zones showed more dependence on the seismic source used to collect the seismic records for the dynamic analysis. This result, not reported in previous studies, means that in sites where the seismic hazard is governed by more than one seismic source that can potentially cause damage to bridges (regions along the Circum-Pacific Belt), overstrength factors in bridge standards could be dependent on the bridges' geographical location. Conversely, the seismic source had moderate relevance on the overstrength factors for bridges located in areas of high seismicity.

The change of the design base shear among the three seismic zones studied was one of the most important parameters in the observed trends of the overstrength factors as a function of the pier height. The application of monotonic load in each direction of analysis independently, commonly used in pushover analyses, overestimated in most cases the overstrength factors determined with time history analysis based on applying simultaneously the three orthogonal components of the seismic movement.

Load combinations for bridges located in high seismicity zones showed that seismic actions have the major impact in the bridge design, and, in these cases, the increase of the pier height had less influence on the overstrength factors. The comparable increase of the design base shear and the base shear capacity in this seismicity zone justified this behavior. However, in cases when gravity loads control the design actions (low seismicity regions for example), the increase of the pier length increases the base shear capacity whereas the design base shear is reduced, and the result is an increase of the bridge overstrength.

Soil-abutment contribution to the bridge capacity in the longitudinal direction led to different trend of the overstrength factors, as compared with the transverse direction where this contribution is negligible. These results were observed in nonlinear static and dynamic analyses.

Finally, the applicability of the results and the proposed equations are limited to the bridge characteristics and seismic parameters comprised in this study. The bridges were reinforced concrete structures with span lengths between 30 and 50 m, pier height in the range of 5–20 m and substructures formed by multi-column piers and single-column piers. However, this group of structures corresponds to the most common bridges found in Mexico and other countries. Although the design of the bridges was carried out for the live loads used in Mexico and the bridges were located in three seismic zones of the Mexican Republic, the general trends may be applicable in other sites of similar seismicity. Due to the importance of overstrength factors in the design of bridges in Mexico and other countries that use force-based design procedures, future studies should analyze bridges on flexible ground sites and include the soil-structure interaction in the linear and nonlinear analyses.

Additionally, future studies could also evaluate the effect of the type of seismic source on the expected seismic response of the bridges by using RotDNN spectra and starting from designing the bridges with the displacement-based philosophy, which allows creating more realistic models, particularly for the inelastic behavior, than bridges designed with the current force-based design philosophy.

Funding

Part of this work reports to research financially supported by Project POCI-01-0145-FEDER- 007457—CONSTRUCT, Institute of R&D in Structures and Construction, funded by FEDER funds through COMPETE2020 and by national funds through Fundação para a Ciência e a Tecnologia (FCT). It was also developed within the scope of the project proMetheus – Research Unit on Materials, Energy and Environment for Sustainability, FCT Ref. UID/05975/2020, financed by national funds through the FCT, MCTES.

Conflicts of interest/Competing interests

The authors have no conflicts of interest to declare that are relevant to the content of this article.

Availability of data and material

Participants of this study did not agree for their data to be shared publicly.

Code availability

Participants of this study did not agree for their code for data to be shared publicly.

Authors' contributions

All authors contributed to the study conception and design. Material preparation, data collection and analysis were performed by Alma R. Sánchez. The first draft of the manuscript was written by Alma R. Sánchez y José M. Jara and all authors commented on previous versions of the manuscript. All authors read and approved the final manuscript.

Ethics approval (Not applicable)

Consent to participate.
All co-authors agree to participate in the research study.

Consent for publication

All co-authors have approved the publication of the manuscript.

Author statement

Alma R. Sánchez: Creation of numerical models, data curation, validation and creation of figures and tables, participation in writing the initial draft.

Antonio Arêde: Formal analysis, data curation, supervision and reviewing the results.

José Jara: Responsible for writing the manuscript, formal analysis, data curation, supervision and reviewing the results.

Pedro Delgado: Formal analysis, data curation, supervision and reviewing the results.

Declaration of competing interest

The authors declare that they have no known competing financial interests or personal relationships that could have appeared to influence the work reported in this paper.

Acknowledgements

The authors gratefully acknowledge the scholarship No. 259 for the first author provided by PRODEP (DSA/103.5/15/9726), and the financial support of the Universidad Michoacana de San Nicolás de Hidalgo, México. Part of this work reports to research financially supported by Base Funding UIDB/04708/2020 and Programmatic Funding - UIDP/04708/2020 of the CONSTRUCT - Instituto de I&D em Estruturas e Construções - funded by Portuguese national funds through the FCT, MCTES (PIDDAC). It was also developed within the scope of the project proMetheus – Research Unit on Materials, Energy and Environment for Sustainability, FCT Ref. UID/05975/2020, financed by national funds through the FCT, MCTES.

References

[1] García D, Singh SK, Herráiz M, Ordaz M, Pacheco JF. Inslab earthquakes in Central Mexico: peak ground-motion parameters and response spectra. Bull Seismol Soc Am 2005;95(6):2272–82.
[2] Frías AR. Disaster experiences in bridges of México. 2014. http://www.amivtac.org/spanelWeb/filemanager/Biblioteca_Amivtac/Seminario-Internacional-Puentes/SIII/SIII-Experiencias-de-Desastres-en-puentes-de-Mexico.pdf. [Accessed 24 November 2020].
[3] MOC. Design Manual of Civil works. Seismic design. México: Electrical Research Institute (IIE); 2015.
[4] Bertero VV, Anderson JC, Krawinkler H, Miranda E. Design guidelines for ductility and drift limits: review of state-of-the-practice and state-of-the-art in ductility and drift-based earthquake-resistant design of buildings. Earthquake Engineering Research Center Report (91/15); 1991.
[5] Park R. Explicit incorporation of element and structure overstrength in the design process. In: Proceedings of the 11th WCEE. IAEE, Acapulco, México; 1996. Paper (2130).
[6] Paulay T. Seismic design of concrete structures the present need of societies. In: Proceedings of the 11th World conference on earthquake engineering. México: Acapulco; 1996.
[7] Luaces FL. Sobrerresistencia de estructuras a base de marcos de concreto reforzado. MSc Thesis. México: División de Estudios de Posgrado, Facultad de Ingeniería, Universidad Nacional Autónoma de México; 1995.
[8] Elnashai AS, Mwafy AM. Overstrength and force reduction factors of multistorey reinforced-concrete buildings. Struct Des Tall Special Build 2002;11(5):329–51.
[9] Varela J, Chan S, Fernández L. Overstrength in autoclaved aerated concrete structures. Ingenieria 2008;12(2):45–55 [in Spanish)].
[10] Miranda E, Bertero VV. The Mexico earthquake of September 19, 1985—performance of low-rise buildings in Mexico City. Earthq Spectra 1989;5(1):121–43.
[11] Shahrooz BM, Moehle JP. Evaluation of seismic performance of reinforced concrete frames. J Struct Eng 1990;116(5):1403–22.
[12] Cassis JH, Bonelli P. Lessons learned from the March 3, 1985 Chile earthquake and related research. In: Proceedings of the 10th World conference on earthquake engineering, Madrid, españa; 1992.
[13] Jain SK, Navin R. Seismic overstrength in reinforced concrete frames. J Struct Eng 1995;121(3):580–5.
[14] Massumi A, Tasnimi AA, Saatcioglu M. Prediction of seismic overstrength in concrete moment resisting frames using incremental static and dynamic analyses. In: Proceedings of the 13th World conference on earthquake engineering. Vancouver, BC: Canada; 2004.
[15] Mehanny SSF, El Howary HA. Assessment of RC moment frame buildings in moderate seismic zones: evaluation of Egyptian seismic code implications and system configuration effects. Eng Struct 2010;32:2394–406.
[16] Khy K, Chintanapakdee C. Quantification of different sources of over-strength in seismic design of a reinforced concrete tall building. Eng J 2019;23(6):1–15.
[17] Kappos AJ, Paraskeva TS, Moschonas IF. Response modification factors for concrete bridges in Europe. J Bridge Eng 2013;18(12):1328–35.
[18] Awasthi J, Ghosh G, Mehta PK. Seismic design of a curved bridge as per performance based criteria. Mater Today Proc 2021;38:3014–8.
[19] Nobuyuki N, Kyeonghoon P, Taiji M, Hiroshige U, Masahide K. Evaluation of seismic performance focusing on increasing response of lead rubber bearing (LRB) and over strength of RC pier during earthquake. Global J Res Eng: Civ Struct Eng 2020;20(3):33–50.
[20] Sánchez AR, Arêde A, Jara JM, Delgado P. Overstrength factors of RC bridges supported on single and multi-column RC piers in Mexico. Earthq Eng Struct Dynam 2021;50(14):3695–712.
[21] Calvi GM, Priestley MJN, Kowalsky MJ. Displacement–based seismic design of structures. In: Proceedings of the 3rd Panhellenic Congress on earthquake engineering and engineering seismology, Athens, Greece; 2008.
[22] Caltrans. Bridge design practice. Seismic design of concrete bridges. Sacramento, California: California Department of Transportation; 2015 [Chapter 21].
[23] Arefi MJ, Pampanin S, Cubrinovski M. Effects of SSI on the seismic response of older structures before & after retrofit. In: Proceedings of the 2009 New Zealand society for earthquake engineering, Christchurch, New Zealand; 2009.
[24] Khosravikia F, Mahsuli M, Ghannad AM. The effect of soil–structure interaction on the seismic risk to buildings. Bull Earthq Eng 2018;16:3653–73.
[25] CSI. SAP2000, V19.2.1 ultimate. Berkeley, California: Computers and Structures, Inc.; 2017.
[26] Mander JB, Priestley JN, Park R. Theoretical stress-strain model for confined concrete. J Struct Eng 1988;114:1804–26.
[27] Park R, Paulay T. Reinforced concrete structures. New York: John Wiley & Sons; 1975.
[28] Paulay T, Priestley MJN. Seismic design of reinforced concrete and masonry buildings. New York: John Wiley & Sons; 1992.
[29] Aashto. AASHTO LRFD bridge design specifications, customary U.S. Units. eighth ed. Washington D.C: American Association of State Highway and Transportation Officials; 2017.